Title

Dynamic Analysis of a Self-Sustainable Renewable Hydrogen Fueling Station

ISBN

978-0-7918-4588-2

Authors

Zhao, Li
Brouwer, Jacob
Samuelsen, Scott

Publication Date

2014-06-30

DOI

10.1115/fuelcell2014-6330

Proceedings of the ASME 2014 12th International Conference on Fuel Cell Science, Engineering and Technology
FUELCELL2014
June 30-July 2, 2014, Boston, Massachusetts, USA

FuelCell2014-6330

DYNAMIC ANALYSIS OF A SELF-SUSTAINABLE RENEWABLE HYDROGEN FUELING STATION

Li Zhao
National Fuel Cell Research Center,
University of California, Irvine
Irvine, CA, U.S.

Jacob Brouwer
National Fuel Cell Research Center,
University of California, Irvine
Irvine, CA, U.S.

Scott Samuelsen
National Fuel Cell Research Center,
University of California, Irvine
Irvine, CA, U.S.

ABSTRACT

To evaluate the dynamic operation and feasibility of designing and operating a self-sustainable hydrogen fueling station using renewable energy sources, system models for a hydrogen fueling station using a proton exchange membrane (PEM) electrolyzer and fuel cell have been developed to simulate the renewable sources and fueling dynamics together with hydrogen production and station operation. Theoretical models have been integrated to simulate station performance when subjected to measured power and fueling demand dynamics from a public fueling station and measured renewable energy supply dynamics. The theoretical models that are integrated into various self-sustainable station design configurations include a Proton Exchange Membrane (PEM) electrolyzer and PEM fuel cell, hydrogen compressor, and storage tank. The fueling dynamics and power consumption dynamics were obtained from an operating public hydrogen fueling station and implemented in the system model. Various control strategies are simulated and the station performance is determined to depend upon the way renewable power is utilized in the station. Due to the round trip efficiency penalty associated with converting electricity to hydrogen (in an electrolyzer) and vice versa (in a fuel cell), the results suggest that the station operation power should be supplied by the renewable sources directly whenever possible, and that the hydrogen fuel cell should provide power only when there is no renewable power available (the third control strategy tested in this paper). The simulated hydrogen fueling station powered by 200 kW wind turbines or 360 kW solar PV were determined to successfully operate in a self-sustainable manner while dispensing ~25 kg of hydrogen per day. This study provides insights regarding the sizing of the station components such as renewable energy conversion devices, electrolyzer and fuel cell, and storage tank. The cost of the hydrogen was determined to be $8.01 per kg when the station is powered by 200 kW of wind turbines and operated using control strategy 3, while it increased to $20.22 per kg when the station is powered by 360 kW of PV array and operated using control strategy 3. This study provides a basis for achieving self-sustainable renewable hydrogen fueling stations. With further optimization and development, these self-sustainable renewable hydrogen fueling stations could provide valuable interconnections (especially in remote locations) throughout the hydrogen infrastructure network and further support the integration of renewable sources for vehicle fuels.

INTRODUCTION

Hydrogen powered fuel cell vehicles are receiving increased attention and automakers have made remarkable advances in fuel cell vehicle development and are projecting initial commercialization in the 2015 timeframe [1]. Currently there are a total of 58 hydrogen fueling stations in the U.S. including private stations, most of which are constructed to support demonstration and research projects that will provide important insights as hydrogen vehicles begin to penetrate the market. With a higher market penetration of hydrogen vehicles in the near future, the hydrogen fueling infrastructure will need to grow substantially to meet the demand. Hydrogen can be produced from various resources via diverse pathways with different levels of emissions associated with each approach [2]. Hydrogen produced by the electrolysis of water with electricity derived from renewable energy sources could potentially eliminate the green-house-gas emissions and air pollution [2-4] from fuel production and delivery. Therefore hydrogen fueling stations powered by renewable sources will not only achieve zero-emission hydrogen production, and support California requirements for 33% renewable hydrogen (Signed into law at

2006, Senate Bill 1505 states that at least 33% of hydrogen produced in California is required to be produced from renewable), but will also significantly extend the existing network of hydrogen fueling stations.

Both experimental and simulation efforts have been carried out by many groups to advance the technology and deployment of hydrogen fueling infrastructure. Such studies have been mainly focused upon: 1) improving electrolysis technology to accommodate renewable hydrogen production, 2) advancing hydrogen storage technology, 3) improving hydrogen production pathways and reducing costs, 4) analyzing and optimizing stand-alone hydrogen production and storage systems, and 5) addressing placement, safety issues, and regulatory policy. Few of these published studies have addressed the dynamic operation of a self-sustainable hydrogen fueling station that considers both renewable source dynamics and fueling dynamics utilizing currently available technologies, as in this effort. However, some recent analyses have addressed related topics. Brown et al. [1] describe a successful public hydrogen fueling station in UC Irvine, that has robustly and safely dispensed 25,000 kg of fuel over the course of 5 years. The average hydrogen consumption is 0.7 kg/car/day and the net station electric use is 5.18 kWh/kg. The net hydrogen cost is also reported as $14.95 per kg of hydrogen. Farzaneh-Gord et al. [5] report a theoretical analysis investigating the performance of hydrogen fuelling stations with different storage types. Two storage types employed have been compared and the results show that the cascade storage type has many advantages over the buffer storage system. The optimized dimensionless low and medium-pressure reservoir pressures are found. Shah et al. [6] describe a conceptual design of a solar powered hydrogen fueling station for a single family home. Sixty high-efficiency PV panels with a total capacity of 18.9 kW account for approximately 94.7% of the hydrogen home's power consumption. The fueling station consists of a 165 bar high pressure electrolyzer for on-site production of 2.24 kg/day of hydrogen, three-bank cascade configuration storage tanks and a hydrogen nozzle. The system produces 0.8 kg/day of hydrogen for a fuel cell vehicle with an average commute of 56 km/day. The energy efficiency obtained by incorporating a solar-hydrogen system for residential applications is also presented. Kelly et al. [4] describe the design and performance of a solar hydrogen fueling station at Milford, MI. The system uses high-efficiency photovoltaic (PV) modules, a high-pressure (6500 psi, 44.8 MPa) electrolyzer, and an optimized direct connection between the PV and electrolyzer systems. It is found that the electrolyzer operated efficiently on solar power over a wide range of conditions and occasional rapidly changing solar radiation and harsh weather conditions won't degrade the system performance. The study estimates that the system could produce approximately 0.5 kg of high-pressure hydrogen per day on solar power for an average summer day in the Detroit area. Dagdougui et al. [7] developed a model consisting of a network of renewable hydrogen fueling stations and several renewable source nodes. The mathematical model gives the selection of the stations that will be powered by each node of renewable sources based on distance and population density criteria, as well as the energy and hydrogen flows exchanged among the system components from the production nodes to the demand points. Rothuizen et al. [8] developed a thermodynamic model to simulate a high pressure hydrogen refueling station and a vehicle storage system. Pressure, temperature and mass flow have been analyzed in the time scale of minutes, and it's shown that the pressure loss in the hydrogen storage system has a significant impact on the hydrogen refueling process in terms of mass flow, cooling demand and storage dimensioning. The results also suggest that cascade fueling reduces compressor work and cooling capacity significantly.

For the purpose of investigating the feasibility of a self-sustainable hydrogen fueling station powered by renewable energy sources, dynamic system models have been developed to simulate the renewable sources and fueling dynamics together with hydrogen production and station operation. Theoretical models have been integrated to simulate station performance when subjected to measured power and fueling demand dynamics from a public fueling station and measured renewable energy supply dynamics. The theoretical models that are integrated into various self-sustainable station design configurations include a Proton Exchange Membrane (PEM) electrolyzer and fuel cell, wind turbines, hydrogen compressor, and storage. The wind speed and solar PV power output are measured from real wind farms and building with PV installation. The station power consumption, hydrogen fueling dynamics are measured from the public hydrogen fueling station in the University of California, Irvine. Analyses include development and evaluation of various control strategies to determine station feasibility and the levelized hydrogen cost estimates. This study presents some valuable insights for designing, sizing, and controlling a self-sustainable renewable hydrogen fueling station.

MODEL DEVELOPMENT

To analyze the feasibility and implications of a self-sustainable hydrogen fueling station using only renewable energy sources, a detailed dynamic system model comprised of renewable energy sources (wind turbines/solar photovoltaic panels) together with hydrogen production, compression, storage and dispatch components is developed in MATLAB/Simulink®. The theoretical models that are integrated into various self-sustainable station design configurations include a Proton Exchange Membrane (PEM) electrolyzer and fuel cell, wind turbines, hydrogen compressor, and storage tank. The wind speed, solar PV power output, fueling station power consumption, and hydrogen fueling dynamics are measured from multiple sources. The performance of a renewable energy source in combination with a PEM electrolyzer and fuel cell, hydrogen compression, storage and dispensing system, form the basis of comparison amongst the various control strategies investigated.

A schematic of the self-sustainable hydrogen fueling station concept using renewable sources that is modeled in this work is presented in Figure 1. In the self-sustainable hydrogen fueling station, renewable energy from the wind turbine or solar PV is directed to the PEM electrolyzer that electrochemically split water into hydrogen and oxygen gases. The hydrogen is compressed and stored in the storage tank for fueling or supplying power to the station. When power is required to meet the station load demand dynamics, either the stored hydrogen is converted back to electrical energy in a PEM fuel cell, or the renewable power is utilized directly, depending upon renewable power availability and the control strategy implemented. The oxygen byproduct is not utilized in this study, but it could also be collected and utilized for various applications. As shown in Figure 1, the public hydrogen fueling station configuration of UC Irvine is utilized in the model, with 35 MPa and 70 MPa fueling and a refrigeration unit.

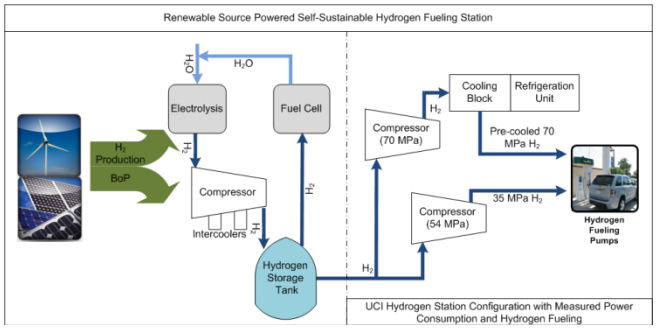

Figure 1. Schematic of a self-sustainable renewable hydrogen fueling station.

System Components: Wind Power Model

Wind power is modeled using wind speed data with ten minute resolution that was obtained from the Wind Integration Datasets provided by the National Renewable Energy Laboratory and 3TIER [9]. Wind speeds were obtained from 50 individual grid points uniformly distributed over approximately 100 square miles in the Plainview, TX region for the current study. Power derived from the wind is determined using equation (1):

$$Power = COP \cdot \frac{1}{2} \rho A v^3 \qquad (1)$$

where *COP* is a coefficient of performance used to match a particular wind turbine's power curve, ρ is the density of air, *A* is the area of the circle swept out by the turbine blades, and *v* is the velocity of the wind. Vestas V47-50 kW wind turbines with a cut-in wind speed of 4 m/s and a cut-out wind speed of 25 m/s were used in the wind turbine model of this study. One week of data, acquired from 6/30/2006 to 7/6/2006 (capacity factor=0.41), comprised the primary input data set for the simulation presented in this study.

System Components: Measured Solar PV Power

The dynamic data for PV power output (kW vs. time (s)) were determined by measurement of a Unisolar 6 kW nominal DC amorphous PV array installed at the University of California, Irvine (Latitude: 33.6 N, Longitude: 117.7 W), on a time interval of every 15 minutes, 24 hours/day [10, 11]. One week of data, acquired from 8/2/2001 to 8/8/2001 (capacity factor=0.22), comprised the primary input data set for the simulation presented in this study. PV technology has been evolved and the conversion efficiency has been improved over the years. However, the data collected and used in the model is representative for the solar radiation conditions.

System Components: Measured Hydrogen Fueling Station Power demand and Hydrogen Dispensed

Hydrogen fueling station power demand was obtained from the public hydrogen fueling station that has been in operation in Irvine, California since 2003. Station electricity consumption was measured as a function of hydrogen dispensed over a week period from 11/4/2012 to 11/10/2012. During this period, 24 kg of hydrogen were dispensed. Current was measured with 30 s resolution at the three-phase, 208 V feed line to the UCI hydrogen station and integrated to give electrical energy for all station loads [1]. The hydrogen station electrical load and the hydrogen dispensed over the week are shown in Figure 2.

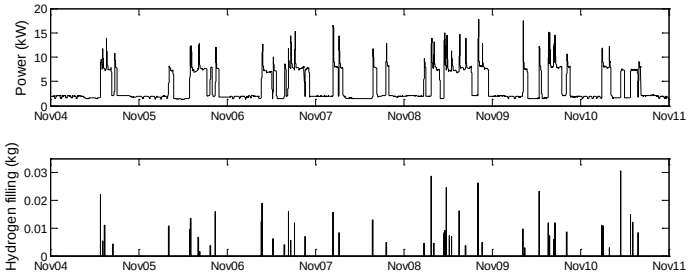

Figure 2. Measured UCI hydrogen station electric load and hydrogen dispensed over a week.

System Components: PEM Electrolyzer Model

The PEM electrolyzer physical model developed in this study is a steady-state model that simulates relations between the cell voltage and cell current that account for activation losses, diffusion losses, and ohmic losses in a PEM electrolyzer stack. The PEM electrolyzer cell voltage is expressed as equation (2), where E is the open circuit voltage, η_{act} is the activation overvoltage, η_{ohm} is the ohmic overvoltage and η_{diff} is the diffusion overvoltage [12, 13]. Using the Nernst equation, the open circuit voltage is calculated by equation (3), where E_{rev}^0 is the reversible cell voltage, R is the gas constant, T is the temperature of the electrolyzer; z is the number of moles of electrons transferred per mole of H_2; F is Faraday's constant; P_{H_2},P_{O_2} and P_{H_2O} are the partial pressures of hydrogen, oxygen, and water, respectively [14, 15]. The activation overpotential is based on electrochemical reaction kinetics and can be deduced from Butler-Volmer equation and rewritten for an electrolyzer as equation (4), where α is the transfer coefficient and i_0 the

exchange current density [12]. The diffusion overpotential is characterized by equation (5), where β is the constant coefficient and i_{lim} the diffusion limit current density [12]. The ohmic overpotential is due to the electrical resistances in the electrolyzer cell that are mainly due to proton conduction resistance in the proton exchange membrane. The ohmic overpotential is given by equation (6), where δ_m is the thickness of the membrane, *A* is the membrane cross-sectional area, σ_m is the conductivity of the proton exchange membrane given by equation (7) proposed by Springer et al. [16], where λ_E is the degree of humidification of the membrane, ranging from 14 (dry enough) to 22 (bathed) [12-15]. In the case of the PEM electrolyzer, the membrane can be considered to be fully hydrated and in this study, λ_E is assumed to be 17 representing good hydration. According to Faraday's Law, the hydrogen production molar flow rate is given by equation (8), where *F* is Faraday's constant [12-15].

$$V_{cell} = E + \eta_{act} + \eta_{ohm} + \eta_{diff} \quad (2)$$

$$E = E_{rev}^0 + \frac{RT}{zF}\ln\left(\frac{P_{H_2}P_{O_2}^{1/2}}{P_{H_2O}}\right) \quad (3)$$

$$\eta_{act} = \frac{RT}{\alpha zF}\ln\left(\frac{i}{i_0}\right) \quad (4)$$

$$\eta_{diff} = \frac{RT}{\beta zF}\ln\left(1 + \frac{i}{i_{lim}}\right) \quad (5)$$

$$\eta_{ohm} = \frac{\delta_m I}{A\sigma_m} \quad (6)$$

$$\sigma_m = (0.005139\lambda_E - 0.00326)exp\left[1268\left(\frac{1}{303} - \frac{1}{T}\right)\right] \quad (7)$$

$$n_{H_2} = \frac{I}{2F} \quad (8)$$

In order to verify the PEM electrolyzer model, experimental data from a 6.5 kW (135A rated, stack voltage=48V) PEM electrolyzer stack from NREL's Wind-to-Hydrogen Project were obtained [17]. Two sets of data were obtained and utilized to verify the model developed in this paper, one for operating at 308 K and 190 psi (1,310 kPa) and one for operating at 328 K and 190 psi (1,310 kPa). The stack current and voltage presented in Figure 3 shows that the model results agree well with the experimental data. In the hydrogen station model, the stack is scaled up to 300 kW rated at 135 A, with 910 electrolysis cells in series operated at 328 K and 200 psi (1,379 kPa).

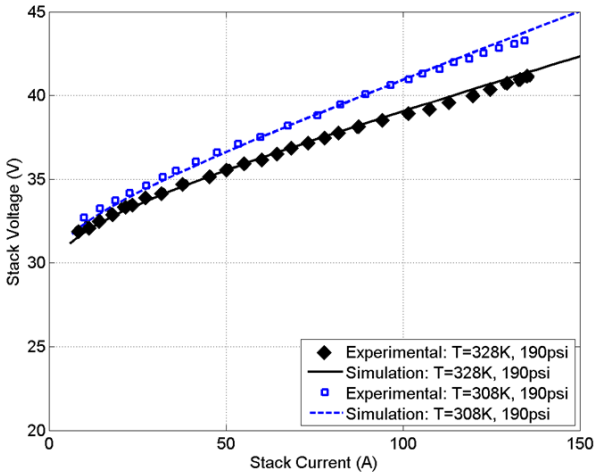

Figure 3. Comparison between current model and experimental data for a 6.5 kW PEM electrolyzer.

System Components: PEMFC Model

The PEM fuel cell physical model developed in this study is a similar steady-state model that simulates relations between the cell voltage and cell current that account for activation losses, concentration losses, and ohmic losses. The PEM fuel cell voltage is expressed as equation (9), where E is the open circuit voltage, η_{act} is the activation overvoltage, η_{ohm} is the ohmic overvoltage and η_{conc} is the concentration overvoltage [18, 19]. Using the Nernst equation, the open circuit voltage is calculated by equation (10), where E_{rev}^0 is the reversible cell voltage, R is the gas constant, T is the temperature of the fuel cell; z is the number of moles of electrons transferred per mole of H_2; F is Faraday's constant; P_{H_2}, P_{O_2}, and P_{H_2O} are the partial pressures of hydrogen, oxygen, and water, respectively [18, 19]. The activation overpotential is based on electrochemical reaction kinetics and can be deduced from Butler-Volmer equation and expressed as equation (11), where α is the transfer coefficient and i_0 the exchange current density [18, 19]. The concentration overpotential is characterized by equation (12), where i_{lim} the limiting current density [18, 19]. The ohmic overpotential is due to the electrical resistances in the fuel cell that mainly contributed from proton exchange membrane. The ohmic overpotential is given by equation (13), where r_m is the resistivity of the proton exchange membrane, and λ_{FC} is the water content of the membrane [19]. Consumption of hydrogen is calculated with Faraday's Law given by equation (8), where n_{H_2} is the number of moles of hydrogen consumed per second.

$$V_{cell} = E - \eta_{act} - \eta_{ohm} - \eta_{conc} \quad (9)$$

$$E = E_{rev}^0 + \frac{RT}{zF}\ln\left(\frac{P_{H_2}P_{O_2}^{1/2}}{P_{H_2O}}\right) \quad (10)$$

$$\eta_{act} = \frac{RT}{\alpha z F} \ln\left(\frac{i}{i_0}\right) \quad (11)$$

$$\eta_{conc} = \frac{RT}{zF} \ln\left(\frac{i_{lim}}{i_{lim} - i}\right) \quad (12)$$

$$\eta_{ohm} = ir_m = i \frac{181.6[1 + 0.03i + 0.062(\frac{T}{303})^2 i^{2.5}]}{(\lambda_{FC} - 0.634 - 3i) exp\left[4.18\left(\frac{T-303}{T}\right)\right]} \quad (13)$$

In order to verify the PEM fuel cell model, experimental data of a 50 cm^2 single cell were obtained [20]. Two sets of data were obtained and utilized to verify the model developed in this paper, one for operating at 363 K and one for operating at 348 K. The polarization curves presented in Figure 4 show that the model results agree well with the experimental data. In the hydrogen station model, the stack is scaled up to 50 kW and operated at 363 K.

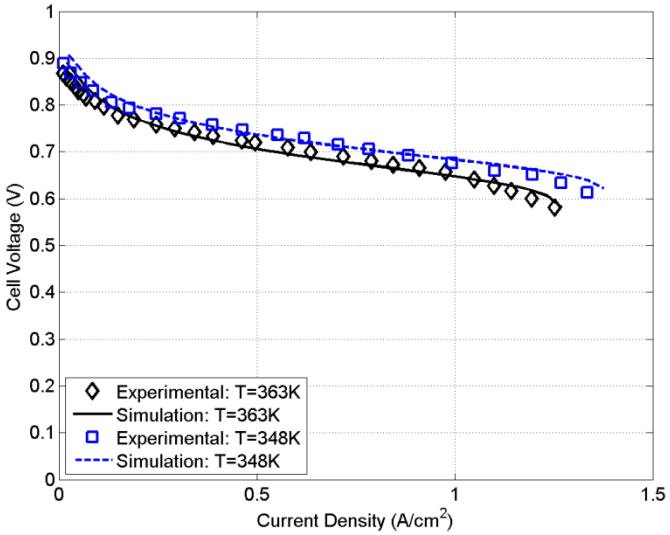

Figure 4. Comparison between modeling and experimental data for the PEM fuel cell.

System Components: Compressor and Storage Tank Model

The hydrogen compressor is modeled with reasonable accuracy by assuming that hydrogen is an ideal gas [21]. The amount of work required to compress hydrogen can be modeled by a polytropic process for the compressor [3, 21-23], using equation (14). The pressure inside the storage tank can be calculated using the ideal gas law of equation (15):

$$W_{comp} = \dot{m}_{H2} w_{comp,in} = \dot{m}_{H2} \frac{nRT_1}{\eta_{comp}(n-1)} \left[\left(\frac{P_2}{P_1}\right)^{(n-1)/n} - 1\right] \quad (14)$$

$$p_{st} = \frac{n_{st} RT}{V_{st}} \quad (15)$$

where W_{comp} is the compressor power in kW, $w_{comp,in}$ is the compressor work in kJ/kg, $\dot{m}_{H2}$ is the hydrogen flow rate in kg/s, T_1 the inlet hydrogen temperature in K, P_1 and P_2 the inlet and outlet hydrogen pressure in kPa, R the hydrogen gas constant of 4.124 kJ/kg* K, n the polytropic coefficient of hydrogen (1.609) and η_{comp} the compressor efficiency, whose value usually ranges between 0.7 and 0.9.

To simulate the dynamics of hydrogen storage tank pressure as it is charged and discharged, the tank and associated piping are taken as a control volume in the model developed. Mass and energy balances are calculated with the following dynamic equations (16) and (17):

$$\frac{dm_{tank}}{dt} = \dot{m}_{in} - \dot{m}_{out} \quad (16)$$

$$\frac{dU_{tank}}{dt} = \dot{n}\bar{h}_{in} - \dot{n}\bar{h}_{out} - \dot{Q} \quad (17)$$

where m_{tank} is the mass of the hydrogen in the storage tank, $\dot{m}_{in}$ and $\dot{m}_{out}$ are the mass flow rates in and out of the tank, U_{tank} is the internal energy of the tank, $\bar{h}$ is the molar specific enthalpy of the hydrogen entering or exiting the storage tank, $\dot{n}$ is the molar flow rate of the hydrogen entering or exiting, and $\dot{Q}$ is the rate of heat transfer into the storage.

Assumptions

The following assumptions are made in the system model:

- Wind turbine is a Vestas model V47 rated at 50 kW.
- η_{comp} = 80%.
- PEM electrolyzer system rated at 300 kW, PEM fuel cell system rated at 50 kW.
- Electrolyzer H_2 outlet pressure of 1,379 kPa (200 psi). [17]
- Maximum allowable hydrogen storage tank pressure is 35 MPa (~5,000 psi).
- Hydrogen Diaphragm Compressor is from Pressure Products Industries model S4000, with discharge pressure up to 103 MPa and hydrogen flow rate up to 85 Nm^3/hr.
- Volume of the hydrogen storage tank is 10 m^3.
- Sufficient ancillary equipment (e.g., switchgear, inverters and converters, small amount of battery storage for inrush currents) with sufficient ramp rates are available to capture excess wind power dynamics as well as provide enough dynamic power during discharge of storage.

RESULTS AND DISCUSSIONS

Control Strategies

Three simple operation and control strategies were implemented in the hydrogen fueling station system model. As described in, the key variances among the control strategies applied are how the station electrical loads were met. The electric demand of the station is comprised of compressor power and station operating/fueling power demands. The electric power is either supplied by the renewable sources directly or by the fuel cell with stored hydrogen as the fuel.

Table 1 – Control strategies tested.	
No.	Control Strategy
1	• Use all renewable power captured to produce hydrogen • Use fuel cell and stored hydrogen to meet the compressor load, and the station fueling load
2	• Use renewable power captured to produce hydrogen and provide power to compress the hydrogen being produced • Use fuel cell and stored hydrogen to meet the station fueling load
3	• Use all renewable power captured to meet the load first, if no renewable power is available, use fuel cell with stored hydrogen to meet the station fueling load • Use the rest of the renewable power captured to produce hydrogen and provide power to compress the hydrogen being produced

To analyze the feasibility and implications of the wind intermittency dynamics, a wind farm with 4 turbines (each rated at 50 kW) has been implemented in the hydrogen fueling station system model. The wind power with a relatively high capacity factor of 0.41 over the course of one week in 2006 is shown in Figure 5. As shown in the figure, the wind power is highly dynamic and varied over the week by a factor of 4. In contrast to the hydrogen dispensing profile showed in Figure 2, the wind power does not exhibit a repeatable diurnal pattern, and large decreases of wind power occur in the middle of the day for most of the days in the week.

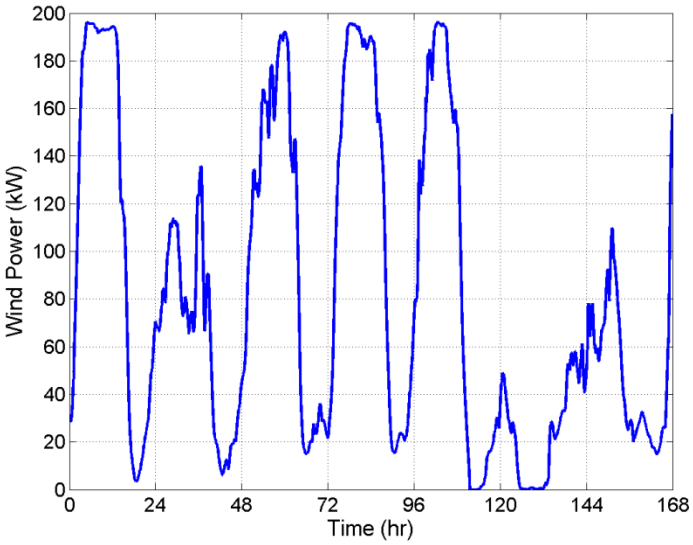

Figure 5. Wind power profile (capacity factor = 0.41), July 2006.

Figure 6 presents the state of charge (SOC) of the hydrogen storage tank for one week of operation using three different control strategies. In the simulation, the fueling station started operating when the SOC is nearly 50%. Operating under all three control strategies, the fueling station was able to supply the hydrogen needed for the vehicles while at least maintaining the initial SOC (~53%) by the end of the week. It is noted that under control strategies 2 and 3, the amount of hydrogen stored was accumulating during the course of the week, and control strategy 3 leads to the highest SOC (80%) at the end of the week. To analyze the dynamics of the production and the consumption, the hydrogen produced from the electrolyzer and consumed in the fuel cell were simulated and shown in Figure 7 and Figure 8, respectively. The system produced a larger amount of hydrogen using control strategy 1 as shown in Figure 7. While operating with control strategy 3, more power was routed to meet the station and compression demand; consequently a lesser amount of hydrogen was produced. As shown in Figure 8, with control strategy 1, the fuel cell consumed a large amount of hydrogen to power the compressor with unavoidable round trip efficiency penalty. As opposed to control strategy 1, much less hydrogen was consumed in the fuel cell using control strategy 3. The overall effect of the imbalance of production and consumption leads to the fact that the control strategy 3 has the best performance over the one week of operation.

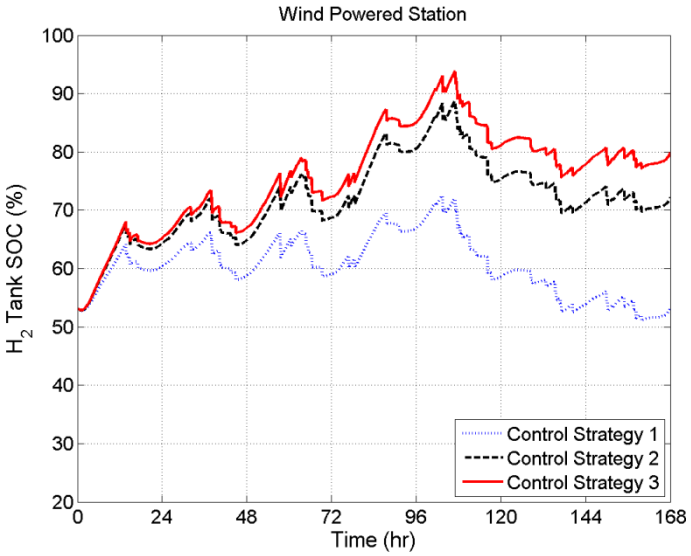

Figure 6. State of charge of the hydrogen storage tank for one week operation, station powered by wind.

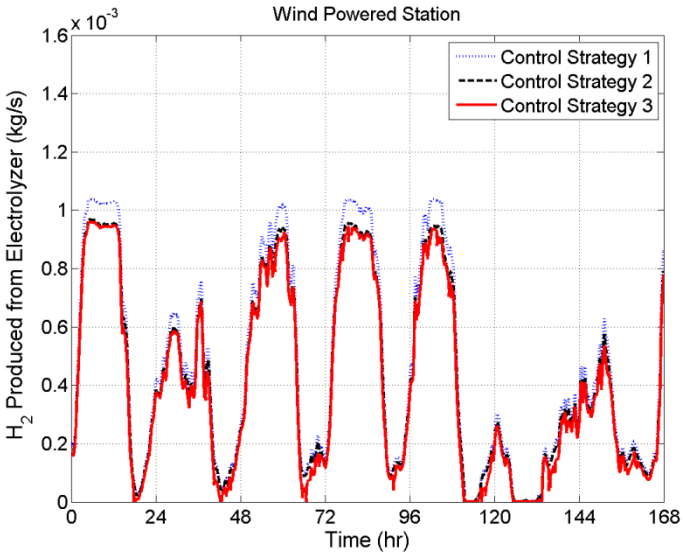

Figure 7. Hydrogen produced from electrolyzer over one week of operation, station powered by wind.

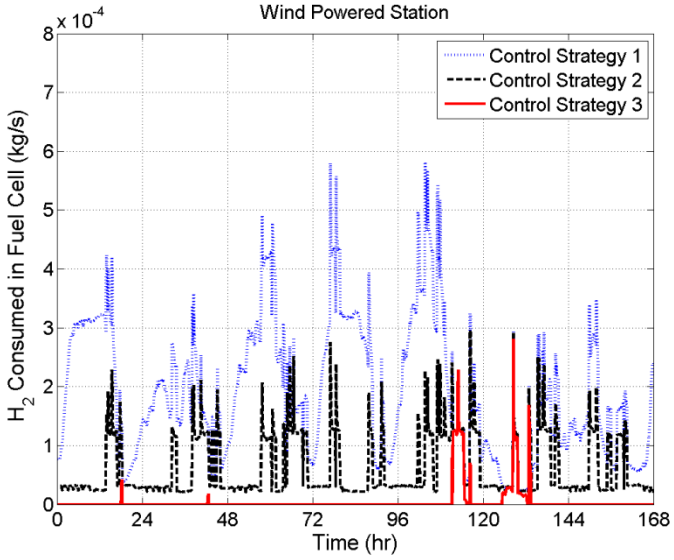

Figure 8. Hydrogen consumed in the fuel cell over one week of operation, station powered by wind.

To analyze the feasibility and implication of the solar PV power dynamics, the self-sustainable station had to be designed with a PV array rated at 360 kW. The solar power data with a capacity factor of 0.22 that occurred over the course of one week in 2001 is shown in Figure 9. As shown in the figure, the solar power exhibits a very consistent diurnal pattern with minimal variations over the course of the week. Compared to the hydrogen dispensing profile shown in Figure 2, the diurnal characteristic of solar power matches well with the fueling activities at the hydrogen station that typically occur during the day time.

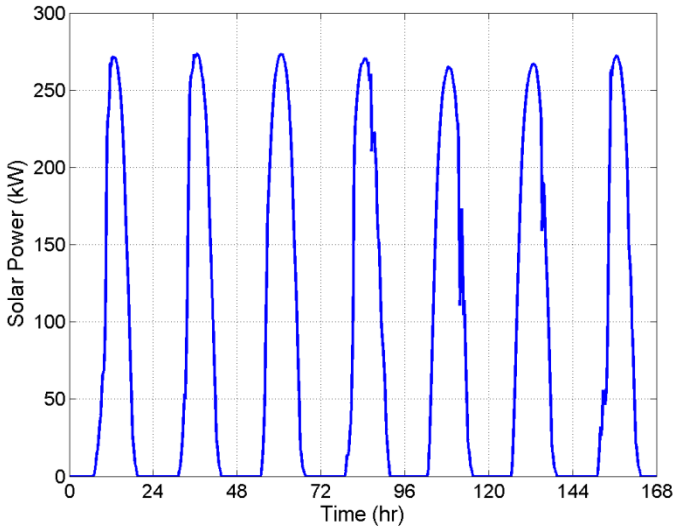

Figure 9. Solar power profile (capacity factor = 0.22), August 2001.

Figure 10 presents the SOC of the hydrogen storage tank for one week of operation using the same three control strategies now with the solar energy source. As with the previous wind power cases, the fueling station started operating when the SOC is nearly 50%. It is noted that under control strategies 2 and 3, the hydrogen storage is accumulating along the course of the week, and control strategy 3 leads to the highest SOC (~72%) at the end of the week. Operating under control strategy 1, after the fueling station supplied the hydrogen needed for the vehicles, the SOC (~49%) at the end of the week is lower than the initial SOC, indicating an imbalance of supply and demand of hydrogen. The hydrogen produced from the electrolyzer and consumed in the fuel cell during this week of operation are shown in Figure 11 and Figure 12, respectively. The system produced a larger amount of hydrogen using control strategy 1, as shown in Figure 11. While operating with control strategy 2 and 3, the amount of hydrogen produced is almost identical. As shown in Figure 12, with control strategy 1 the fuel cell consumed a large amount of hydrogen to power the compressor and a much smaller amount of hydrogen is needed using control strategy 3. It is also noted that when the station is powered by solar energy sources, all control strategies are required to consume the same amount of hydrogen to provide the base load of the fueling station during night time (mostly for lighting at the station).

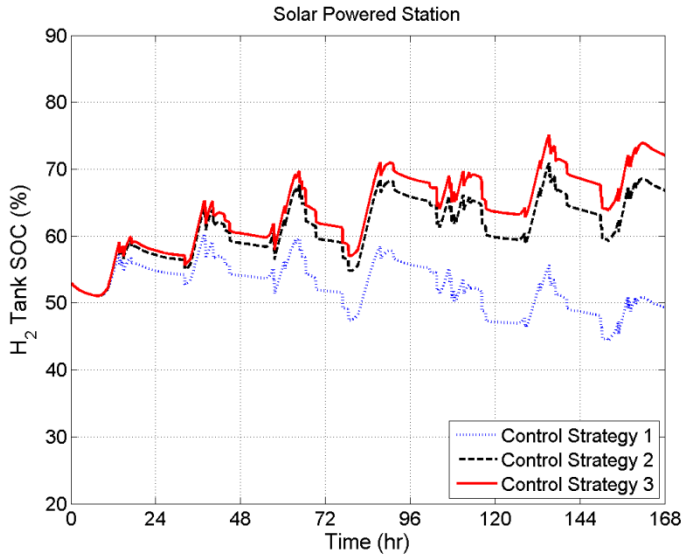

Figure 10. State of charge of the hydrogen storage tank for one week operation, station powered by solar PV.

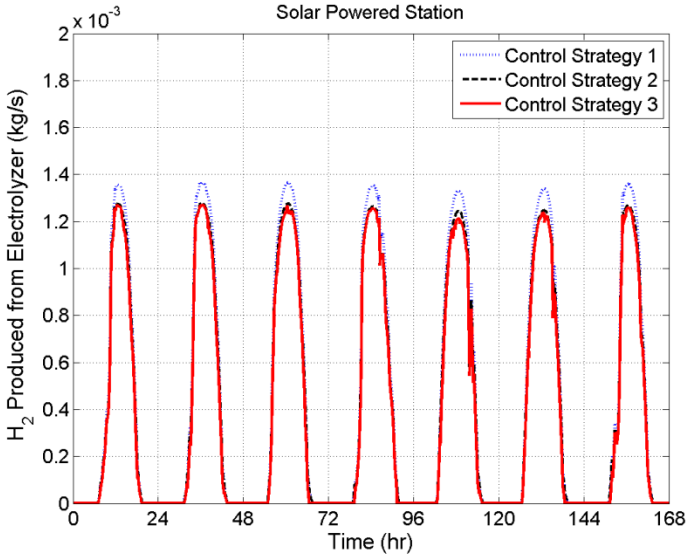

Figure 11. Hydrogen produced from electrolyzer over one week of operation, station powered by solar PV.

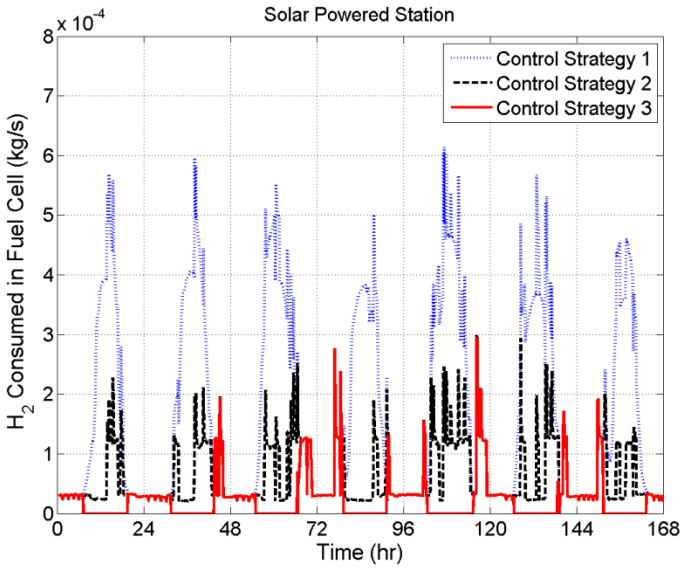

Figure 12. Hydrogen consumed in the fuel cell over one week of operation, station powered by solar PV.

Energy Fluxes

To compare the station performance using different renewable energy sources, and provide a full view of energy fluxes, Sankey diagrams are shown in Figure 13 for control strategy #3. The width of the arrows corresponds to the amount of energy associated with each flux. Over the course of the week, total wind energy input to the system is 13,538.5 kWh and total solar energy input to the system is 13,488.2 kWh, with a difference of less than 0.4%. For all cases, the initial hydrogen energy in the storage is 5,012.8 kWh (LHV), and the fueling output is 5,340 kWh (LHV).

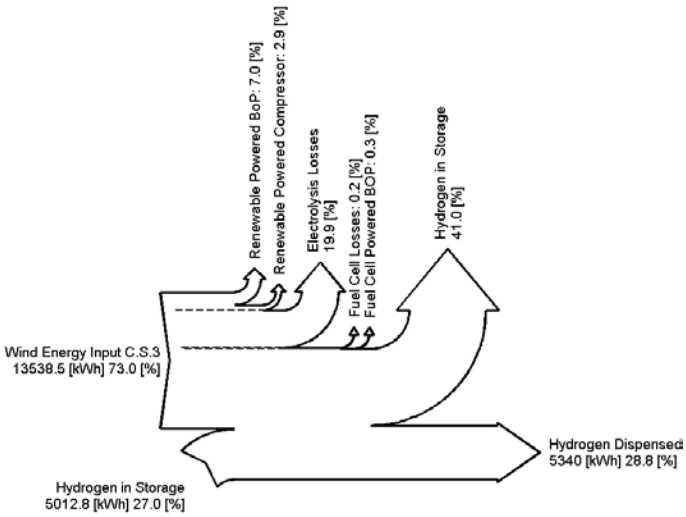

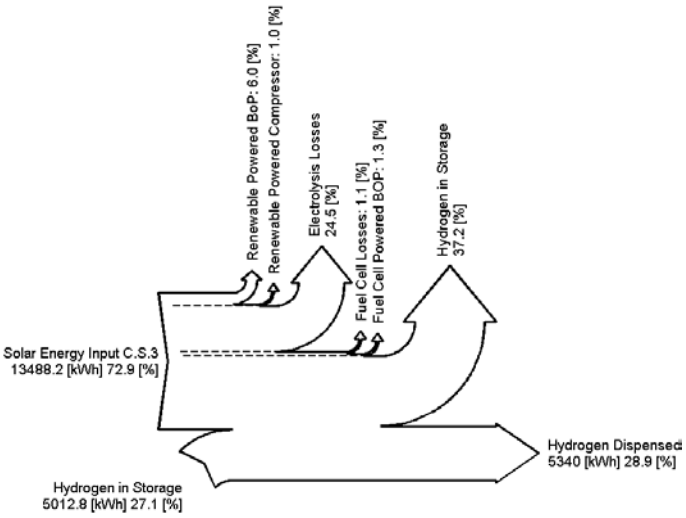

Figure 13. Sankey diagrams of energy fluxes for wind and solar powered stations using control strategy 3.

Cost of Hydrogen

The per kilogram cost of hydrogen is evaluated based upon the self-sustainable fueling station model of this study. The cost of hydrogen is evaluated based upon a number of factors including control strategy, capacity factor, levelized renewable energy cost, levelized cost of PEM fuel cell and electrolyzer, compressor, storage, dispenser and BoP of the fueling station. The detailed hydrogen production cost contributions are presented in Table 2. The cost of a net 80-kW PEM fuel cell system based on 2012 technology and operating on direct hydrogen is projected to be $84/kW when manufactured at a volume of 10,000 units per year [24]. The cost of a 50 kW PEM fuel cell system with 10,000 hours lifetime is evaluated based on these values.

Powered by 200 kW of wind turbines and operated using control strategy 3, the cost of hydrogen is $8.01 per kg, as powered by 360 kW of PV array and operated using control strategy 3, the cost of hydrogen is $20.22 per kg. According to the U.S. Department of Energy, the cost of centralized or distributed hydrogen production from wind has 2015 targets of $3.10/kg and $3.70/kg, respectively [25]. However, the costs of hydrogen produced by the self-sustainable hydrogen fueling station simulated in this study ($8.01/kg-$H_2$ and $20.22/kg-$H_2$) are comparable to the cost of hydrogen dispensed at the current UCI hydrogen fueling station ($14.94/kg-$H_2$) [1].

Table 2 – Hydrogen production cost contribution.

Levelized Energy Cost ($/kWh)		Levelized Capital Cost ($/kWh)	Levelized Hydrogen Cost ($/kg-$H_2$)
Wind [25-28]	Solar PV [26]	PEM Fuel Cell [24]	PEM Electrolyzer [29]
0.100	0.280	0.42	0.700

Levelized Cost, portion of Compressor, Storage, and Dispensing ($/kg-$H_2$) [27, 30]			
Compressor	Storage	Dispenser	
0.498	0.825	0.083	
Refrigeration		Remainder of Station	Total
0.115		0.008	1.529

SUMMARY AND CONCLUSIONS

To evaluate the dynamic operation and feasibility of designing and operating a self-sustainable hydrogen fueling station using renewable energy sources, system models have been developed to simulate the renewable sources and fueling dynamics together with hydrogen production and station operation. Theoretical models have been integrated to simulate station performance when subjected to measured power and fueling demand dynamics from a public fueling station and measured renewable energy supply dynamics. Various control strategies are simulated and the station performance is determined to depend upon the way renewable power is utilized in the station. Due to the round trip efficiency penalty associated with converting electricity to hydrogen (in an electrolyzer) and vice versa (in a fuel cell), the results suggest that the station operation power should be supplied by the renewable sources directly whenever possible, and that the hydrogen fuel cell should provide power only when there is no renewable power available. The simulated hydrogen fueling station powered by 200 kW wind turbines or 360 kW solar PV were determined to successfully operate in a self-sustainable manner while dispensing ~25 kg of hydrogen per day. The cost of the hydrogen was determined to be $8.01 per kg when the station is powered by 200 kW of wind turbines and operated using control strategy 3, while it increased to $20.22 per kg when the station is powered by 360 kW of PV array and operated using control strategy 3.

Although the wind power and solar PV power profile used in this study were collected during one week, the capacity factors of the renewable sources were representative. To further investigate the performance of the self-sustained hydrogen fueling station, renewable power profile with longer duration and various capacity factors need to be implemented in the model. In addition, the hydrogen fueling pattern also needs to

be implemented to the model with longer durations, to find out the impact of fueling patterns on the station performance.

This study provides a basis for achieving self-sustainable renewable hydrogen fueling stations. With further optimization and development, these self-sustainable renewable hydrogen fueling stations could provide valuable interconnections (especially in remote locations) throughout the hydrogen infrastructure network and further support the integration of renewable sources for vehicle fuels.

ACKNOWLEDGMENTS

The authors would like to thank Dr. Tim Brown, Richard Hack, and Jean Grigg from Advanced Power and Energy Program, University of California, Irvine, for their technical support.

REFERENCES

[1] Brown, T., Stephens-Romero, S., and Scott Samuelsen, G., 2012, "Quantitative analysis of a successful public hydrogen station," International Journal of Hydrogen Energy, 37(17), pp. 12731-12740.

[2] Lee, J.-Y., An, S., Cha, K., and Hur, T., 2010, "Life cycle environmental and economic analyses of a hydrogen station with wind energy," International Journal of Hydrogen Energy, 35(6), pp. 2213-2225.

[3] Dursun, E., Acarkan, B., and Kilic, O., 2012, "Modeling of hydrogen production with a stand-alone renewable hybrid power system," International Journal of Hydrogen Energy, 37(4), pp. 3098-3107.

[4] Kelly, N., Gibson, T., and Ouwerkerk, D., 2008, "A solar-powered, high-efficiency hydrogen fueling system using high-pressure electrolysis of water: Design and initial results," International Journal of Hydrogen Energy, 33(11), pp. 2747-2764.

[5] Farzaneh-Gord, M., Deymi-Dashtebayaz, M., Rahbari, H. R., and Niazmand, H., 2012, "Effects of storage types and conditions on compressed hydrogen fuelling stations performance," International Journal of Hydrogen Energy, 37(4), pp. 3500-3509.

[6] Shah, A., Mohan, V., Sheffield, J. W., and Martin, K. B., 2011, "Solar powered residential hydrogen fueling station," International Journal of Hydrogen Energy, 36(20), pp. 13132-13137.

[7] Dagdougui, H., Ouammi, A., and Sacile, R., 2012, "Modelling and control of hydrogen and energy flows in a network of green hydrogen refuelling stations powered by mixed renewable energy systems," International Journal of Hydrogen Energy, 37(6), pp. 5360-5371.

[8] Rothuizen, E., Mérida, W., Rokni, M., and Wistoft-Ibsen, M., 2013, "Optimization of hydrogen vehicle refueling via dynamic simulation," International Journal of Hydrogen Energy, 38(11), pp. 4221-4231.

[9] Maton, J.-P., Zhao, L., and Brouwer, J., 2013, "Dynamic modeling of compressed gas energy storage to complement renewable wind power intermittency," International Journal of Hydrogen Energy, 38(19), pp. 7867-7880.

[10] Maclay, J. D., Brouwer, J., and Samuelsen, G. S., 2007, "Dynamic modeling of hybrid energy storage systems coupled to photovoltaic generation in residential applications," Journal of Power Sources, 163(2), pp. 916-925.

[11] Maclay, J. D., Brouwer, J., and Samuelsen, G. S., 2011, "Experimental results for hybrid energy storage systems coupled to photovoltaic generation in residential applications," International Journal of Hydrogen Energy, 36(19), pp. 12130-12140.

[12] Lebbal, M. E., and Lecœuche, S., 2009, "Identification and monitoring of a PEM electrolyser based on dynamical modelling," International Journal of Hydrogen Energy, 34(14), pp. 5992-5999.

[13] Marangio, F., Santarelli, M., and Cali, M., 2009, "Theoretical model and experimental analysis of a high pressure PEM water electrolyser for hydrogen production," International Journal of Hydrogen Energy, 34(3), pp. 1143-1158.

[14] Awasthi, a., Scott, K., and Basu, S., 2011, "Dynamic modeling and simulation of a proton exchange membrane electrolyzer for hydrogen production," International Journal of Hydrogen Energy, 36(22), pp. 14779-14786.

[15] Gorgun, H., 2006, "Dynamic modelling of a proton exchange membrane (PEM) electrolyzer," International Journal of Hydrogen Energy, 31(1), pp. 29-38.

[16] Springer, T. E., Zawodzinski, T. A., and Gottesfeld, S., 1993, "Polymer Electrolyte Fuel Cell Model," Journal of Electrochemcal Society, 138(8), pp. 2334-2342.

[17] Harrison, K. W., Martin, G. D., and Ramsden, T. G., 2009, "The Wind-to-Hydrogen Project : Operational Experience , Performance Testing , and Systems Integration The Wind-to-Hydrogen Project : Operational Experience , Performance Testing , and Systems Integration," Golden, Colorado.

[18] Kuo, J.-K., and Wang, C.-F., 2011, "An integrated simulation model for PEM fuel cell power systems with a buck DC–DC converter," International Journal of Hydrogen Energy, 36(18), pp. 11846-11855.

[19] Musio, F., Tacchi, F., Omati, L., Gallo Stampino, P., Dotelli, G., Limonta, S., Brivio, D., and Grassini, P., 2011, "PEMFC system simulation in MATLAB-Simulink® environment," International Journal of Hydrogen Energy, 36(13), pp. 8045-8052.

[20] Ahluwalia, R. K., Lajunen, X. W. A., Wang, X., and Kumar, R., 2012, "Fuel Cells Systems Analysis, 2012 DOE Hydrogen Program Review," Washington, DC.

[21] Deshmukh, S. S., and Boehm, R. F., 2008, "Review of modeling details related to renewably powered hydrogen systems," Renewable and Sustainable Energy Reviews, 12(9), pp. 2301-2330.

[22] Carapellucci, R., and Giordano, L., 2012, "Modeling and optimization of an energy generation island based on

renewable technologies and hydrogen storage systems," International Journal of Hydrogen Energy, 37(3), pp. 2081-2093.
[23] Raju, M., and Khaitan, S. K., 2012, "System simulation of compressed hydrogen storage based residential wind hybrid power systems," Journal of Power Sources, 210, pp. 303-320.
[24] Spendelow, J., and Marcinkoski, J., 2012, "DOE Fuel Cell Technologies Program Record: Fuel Cell System Cost."
[25] Saur, G., and Ainscough, C., 2011, "U . S . Geographic Analysis of the Cost of Hydrogen from Electrolysis U . S . Geographic Analysis of the Cost of Hydrogen from Electrolysis," Golden, Colorado.
[26] "Transparent Cost Database/Open Energy Information."
[27] Genovese, J., Harg, K., Paster, M., and Turner, J., 2009, "Current (2009) State-of-the-Art Hydrogen Production Cost Estimate Using Water Electrolysis Independent Review," Golden, Colorado.
[28] Saur, G., and Ramsden, T., 2011, "Wind Electrolysis : Hydrogen Cost Optimization Wind Electrolysis : Hydrogen Cost Optimization," Golden, Colorado.
[29] Hamdan, M., 2012, "2012 Hydrogen Program Annual Merit Review Meeting: PEM Electrolyzer Incorporating an Advanced Low Cost Membrane."
[30] "DOE H2A Production Analysis," http://www.hydrogen.energy.gov/h2a_production.html.